Application of high frequency biasing and its effect in STOR-M tokamak

Application of high frequency biasing and its effect in STOR-M tokamak

Debjyoti Basu[a,b], Masaru Nakajima[a], A.V. Melnikov[c,d], Julio J. Martinell[e], David McColl[a], Raj Singh[b], Chijin Xiao[a], Akira Hirose[a]
[a] *Plasma Physics Laboratory, University of Saskatchewan, 116 Science Place, Saskatoon, SK, S7N5E2, Canada*
[b] *Present address: Institute for Plasma Research, Bhat, Gandhinagar-382428, India**
[c] *NRC Kurchatov Institute, 123182, Moscow, Russia*
[d] *National Research Nuclear University MEPhI, 115409, Moscow, Russia and*
[e] *Instituto de Ciencias Nucleares-UNAM, Mexico D.F. 04510, Mexico*†

(Dated: May 9, 2020)

Abstract

A pulsed oscillating power amplifier has been developed to apply high frequency biasing voltage to an electrode at the edge of the STOR-M tokamak plasma. The power amplifier can deliver a peak-to-peak oscillating voltage ±60V and current 30A within the frequency range 1kHz-50kHz. The electrode is located in the equatorial plane at radius $\rho = 0.88$. The frequency of the applied voltage has been varied between discharges. It is observed that the plasma density and soft x-ray intensity from the plasma core region usually increase at lower frequency regime 1kHz-5kHz as well as relatively higher frequency regime 20kHz-25kHz but seldom increase in between them. Increment of τ_E has been observed 40% & 20% for 1kHz-5kHz & 20kHz-25kHz respectively and τ_p increment is 25% for both frequency regimes. Transport simulation has been carried out using the ASTRA simulation code for STOR-M tokamak parameters to understand the physical process behind experimental observations at the higher frequency branch. The model is based on geodesic acoustic mode(GAM) excitement at resonance frequency associated with Ware-pinch due to oscillating electric field produced by biasing voltage which can suppress anomalous transport. Simulation results reproduce the experimental trends quite well in terms of the density, particle confinement as well as energy confinement time evolution. All those results indicate that high frequency biasing is capable of improving confinement efficiently.

Edge plasma turbulence in tokamak plays a crucial role in plasma transport and confinement [1]. In general, it is believed that anomalous transport in tokamaks is governed by plasma turbulence. Experimentally, it has been established that anomalous transport happens mostly due to edge electrostatic turbulence [2, 3], but the basic mechanism of edge turbulence is not clear till now. Another interesting feature of turbulence phenomena is the possibility to drive zonal flows and geodesic acoustic mode(GAM) [4, 5] when it reaches certain energy level and may help to trigger H-mode in a tokamak. Turbulence has an interesting nature and a great importance related to tokamak plasma confinement where it generally worsens plasma confinement but sometimes deterioration is reduced, leading to a relatively better plasma confinement. Therefore, high frequency biasing [6] may be another approach for understanding the role of turbulence in plasma confinement.

Previously, a series of dc and low frequency (around few hertz) ac electrode biasing [7–12] and turbulent feedback experiments [13–15] have been performed to understand the nature of anomalous transport and improved confinement achieved by edge turbulence suppression. Recently, it was planned to perform high frequency (kilo-Hertz range), electrode biasing experiments on the STOR-M tokamak to study the dependency of transport on biasing voltage frequency. So, an ac broadband (1kHz-50kHz) power amplifier has been developed to meet the experimental needs to amplify a broadband signal without phase shift.

In this paper, a brief description of the power amplifier development, the experimental results and the analysis of its physical nature through transport simulation using the ASTRA code will be discussed.

The STOR-M tokamak is a limiter based small tokamak with circular plasma cross-section having major and minor radii 46cm and 12cm respectively. In high-frequency biasing experiments, an oscillating voltage of ±60V has been applied by the developed power amplifier at the plasma edge through an electrode made of rectangular stainless steel plate located in the equatorial plane at a plasma radius of $10.5(\rho = 0.88)$cm. The frequency of the applied voltage has been varied from 1kHz to 25kHz on a shot to shot basis in this experiment, based on previous frequency scanning results where they showed that there were very rare changes of density as well as H_α intensity compared with cases without bias above 25kHz. A 12 channel pin-hole soft x-ray camera masked by a 1.8μm aluminum foil and viewed from a top port[16] has been used to measure line-integrated soft x-ray emission intensity. A half-meter monochromator for H_α recording and a 4mm microwave interferometer for line averaged electron density measurement have been used.

The power amplifier can deliver an output signal with peak voltage ±60V and maximum current 30A without any distortion in any waveform within the frequency range 1kHz-50kHz when its input voltage and current are 0.25V & 0.5A respectively. The selected frequency range has been chosen based on the dominant frequency of the

*Electronic address: debjyotibasu.basu@gmail.com
†Electronic address: martinel@nucleares.unam.mx

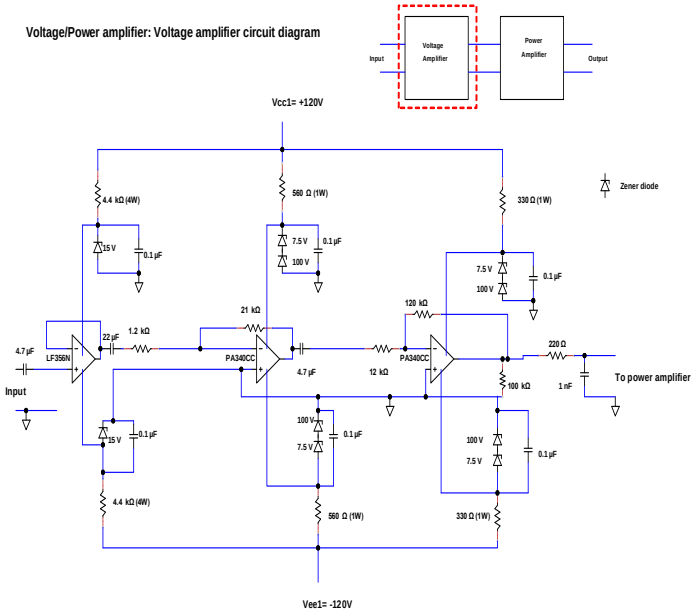

FIG. 1: Voltage amplifier section.

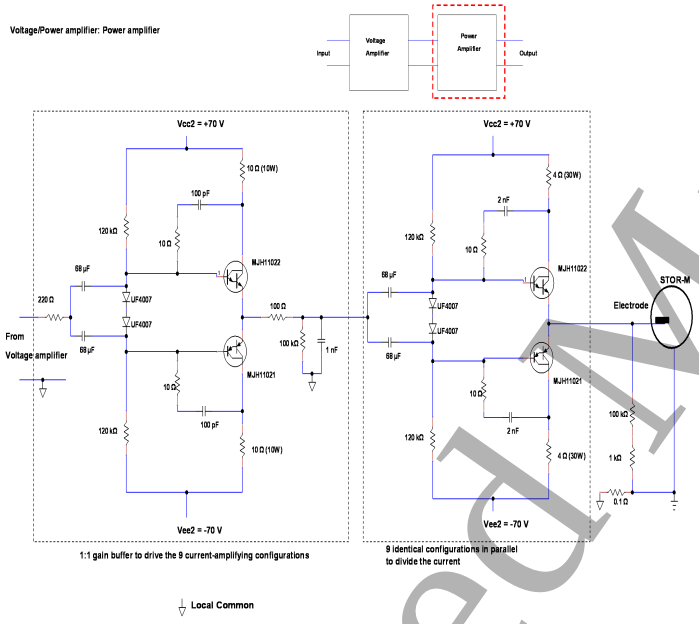

FIG. 2: Current amplifier section.

drift mode driven by density gradients present in STOR-M. The power amplifier has two key parts which amplify voltage(figure 1) & current(figure 2) and thus the overall power of a waveform. Voltage amplification has been done through a high frequency and power MOSFET op-amp PA340CC. Voltage has been amplified by two inverting op-amp amplifiers with resultant amplification factor around 175. MJH11021 PNP and MJH11022 NPN darlington pairs with ratings 250V & 10A have been used for current amplification. Nine identical push-pull amplifiers are connected in parallel to deliver the combined high power required for the experiments. A voltage divider and a 0.1Ω sampling resistor are used to monitor electrode voltage and current through the plasma. The power amplifier is gated and driven by a function generator. Activation and operational time duration of the amplifier is controlled by a pulsed controller circuit using solid state analog switch LF13202. The pulsed controller circuit is turned on by a master optical trigger pulse. Pulse delay and its width can be varied from 0.5ms-44ms and 1ms-45 ms, respectively.

Frequency was varied between shots from 1kHz to 25kHz. Interestingly, biasing improves confinement for frequency regimes of 1kHz-5kHz & 20kHz-25kHz. The confinement was rarely improved outside these two frequency regimes. A typical plasma shot with and without biasing is shown in figure 3.

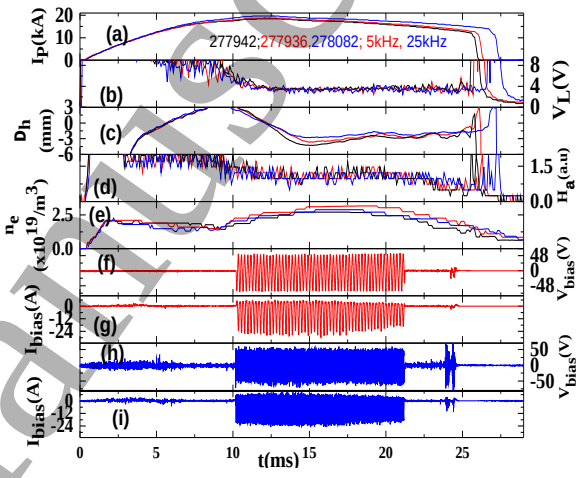

FIG. 3: Temporal evolution of plasma parameters without (black line) & with (red line 5kHz & blue line 22kHz) biasing (a) plasma current, (b) loop voltage, (c) plasma horizontal position, (d) Plasma H_α intensity, (e) line averaged density, (f) bias voltage, (g) bias current at low frequency; (h) bias voltage, (i) bias current at high frequency.

In this typical example, a triangular voltage signal with peak to peak voltage of ±60V was applied from 10ms to 21ms at 5kHz & 25kHz during the plateau of the STOR-M discharge current as shown in figure 3. Here, an important feature is that the overall plasma density has increased without a significant change in H_α intensity, as shown in figure 3(d) & 3(e). Horizontal equilibrium plasma position started to shift during application of the high frequency bias voltage but came back to its equilibrium position due to the position feedback control, as seen in figure 3(c). Interestingly, figure 3(f), 3(g), 3(h) & 3(i) shows that the maximal value of the electrode current decreases with time while the electrode voltage remains unchanged indicating improved confinement[7, 17].

Time evolution of the central soft x-ray channel signal and the particle confinement time (τ_p) with and without biasing are presented in figure 4(a) & 4(b). τ_p is the ratio of electron density n_e to H_α intensity[18], which is

enhanced due to biasing. Increment of soft x-ray signals from the central and its adjacent channels has been noticed from the radial profile in presence of biasing in time window 15.5ms-16.5ms, as shown in figure 4(c).

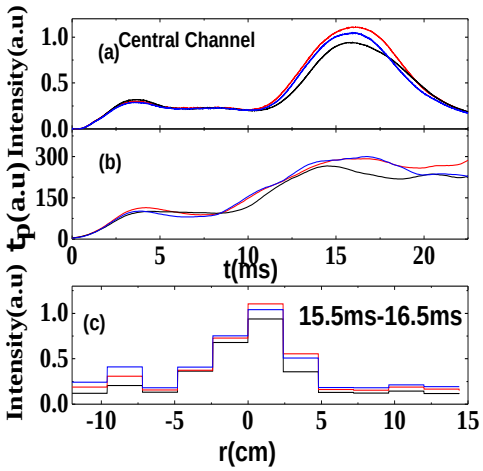

FIG. 4: Temporal evolution of (a) soft x-ray central channel, (b)representation of particle confinement time, (c)radial profile of soft x-rays intensity averaged over $15.5ms - 16.5ms$ with(red line 5kHz & blue line 22kHz) & without(black line) bias.

These results indicate that an improvement of core plasma confinement may happen due to biasing. The nature of density variation and soft x-ray behaviour at different frequencies is shown in figure 5. Interestingly, it is observed in figure 5(a) & 5(b) that changes are sometimes opposite in soft x-ray and density time profiles with different bias frequencies. If density is lower at lower frequency then soft x-ray intensity is higher at lower frequency compared to that at higher frequency. In this typical example, density and soft x-ray profiles at 3kHz, 20kHz & no bias are compared. To quantify the differences, a percentage increment of $n_e.T_e$(a.u) has been derived within 15.5ms-18.5ms at lower frequencies (1kHz-5kHz) as well as in higher frequencies (20kHz-25kHz) where the maximum change happened for both profiles. Soft x-ray intensity has been used for the derivation of percentage increment of $n_e.T_e$(a.u) assuming that it is all due to bremsstrahlung radiation. This radiation, which is received by soft x-ray detectors, can be written as $I_{br} = cn_e^2 T_e^{1/2} Z_{eff}$ [19], where, I_{br}, n_e, T_e are in watt/m^3,m^{-3}, eV respectively and 'Z_{eff}' is the effective ion charge state. Here, it is considered that 'Z_{eff}' remains unaltered in both situations for different frequencies because comparison between the cases with & without bias shows that I_p does not decrease and V_L & H_α do not increase. As a good approximation, it can be concluded that $n_e.T_e \propto I_{br}^2/n_e^3$.

Smoothed signals of V_L & H_α using adjacent averaging of 25 points have been plotted in figure 6(a) & 6(b) within

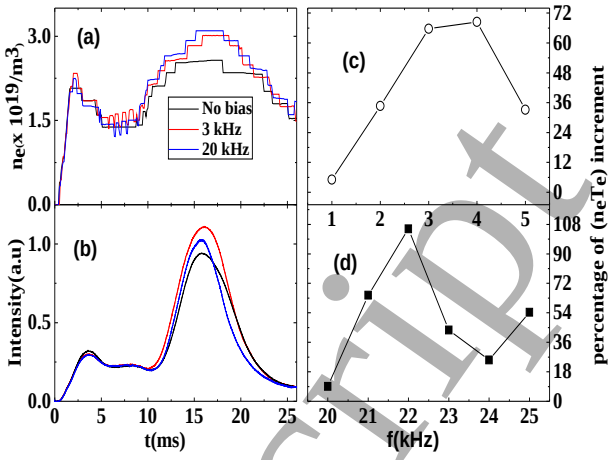

FIG. 5: Temporal evolution of (a) density, (b) soft x-ray central channel at without bias (black), with 3kHz(red) and 20kHz(blue) bias, frequency dependence of percentage increment of $n_e.T_e$ at (c) lower frequency branch, (d) higher frequency branch.

time window of 12ms-24ms. V_L and H_α profiles within 15.5ms-18.5ms clearly show that they are decreased with biasing. Intensity coming from the same soft x-ray channel has been compared for the cases with and without bias. Since, soft x-ray radiation comes from around the plasma center, density value from interferometer data is used for getting a crude approximation. Here, percentage increment of a physical quantity 'α' is defined as $\frac{\alpha_{withbias} - \alpha_{withoutbias}}{\alpha_{withoutbias}} \times 100$. Energy percentage increment reaches maximum at 4kHz & 22kHz as shown in figure 5(c) & 5(d). The increment of n_eT_e is an indication of plasma beta enhancement which is supported by Grad-Shafranov shifting of plasma column horizontally from its equilibrium position as shown in figure 6(c).

Percentage increment of τ_p & a new physical quantity τ_E_I_{soft} are shown in figure 7(a)& 7(b)for lower and higher frequency regimes respectively, where $\tau_{E\_}I_{soft} \propto \frac{I_{br}^2}{n_e^3 I_p V_L}$ and $\tau_p \propto \frac{n_e}{H\alpha}$. It is noticed that the shape of frequency profiles of τ_p and τ_E_I_{soft} look apparently almost the same in the lower frequency branch as well as in the higher frequency branch.

τ_E has also been derived from $\tau_{E\_}kinetic \approx \frac{<n_e><T_e>v_{plasma}}{I_P V_L}$. The percentage increment of τ_E_I_{soft} & τ_E_kinetic have been plotted in figure 8(a) & 8(b) for lower and higher frequency regimes respectively. Interestingly, the frequency profiles of τ_E_I_{soft} & τ_E_kinetic increments at low frequency regime look the same and have the peak value at the same frequency (2kHz). On the other hand, the frequency profile of the τ_E_kinetic increment is oscillatory in the high frequency regime which is unlike the τ_E_I_{soft} increment frequency profile, as clearly seen in figure 8(b). It needs to be mentioned that energy confinement time calculations from τ_E_kinetic (conven-

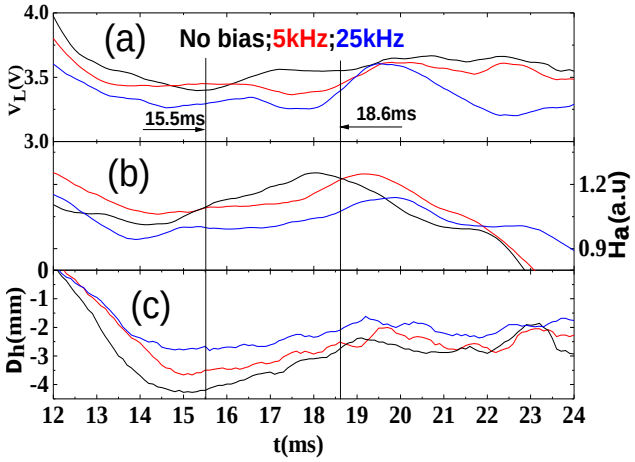

FIG. 6: Temporal evolution of zoomed (a) loop voltage (smoothed 25 points), (b) H_α-intensity (smoothed 25 points), (c)horizontal position (Δ_h) at without bias(black), with 5kHz(red) and 25kHz(blue)bias.

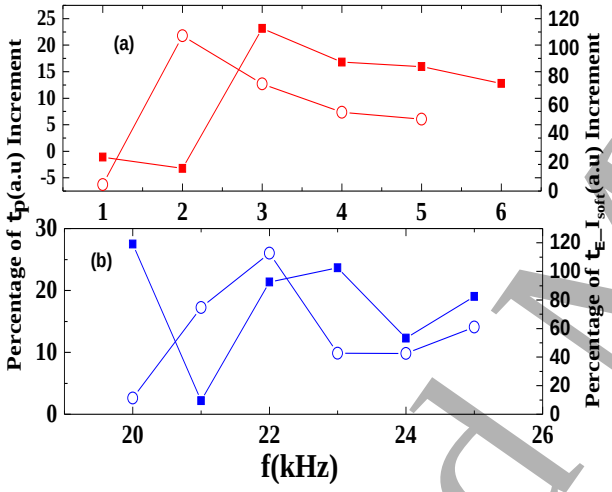

FIG. 7: Percentage increment of τ_p (solid square box) & τ_E (hollow circle) (a) lower frequency branch (red line), (b) higher frequency branch(blue line).

tional method) and $\tau_{E\_I_{soft}}$ (new definition) predict the same frequency peak but their magnitudes differ by factors 3-5 times. The factor of difference arises probably due to different causes like (1)the soft X-ray emission includes not only bremsstrahlung radiation, as it was assumed, but also some contributions from line radiation and (2)$\tau_{E\_I_{soft}}$ is more a local measurement around central plasma region while $\tau_{E_}$kinetic is a plasma volume averaged quantity.

In order to understand the inherent physics of improved confinement, possible mechanisms related to the effect of AC biased electrode have been explored. Since

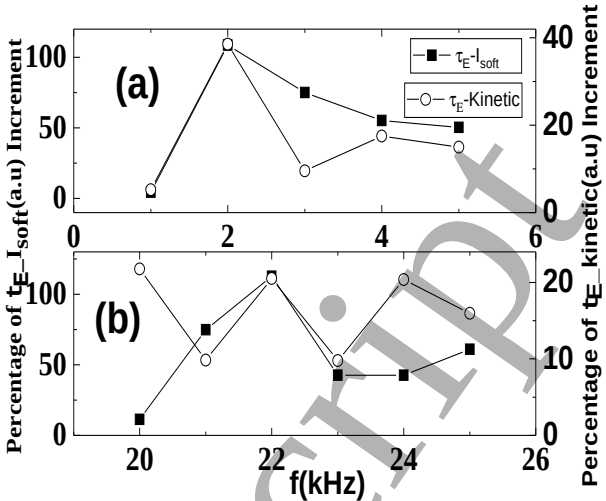

FIG. 8: Comparison between percentage increment of $\tau_{E\_}I_{Soft}$(solid square box) & $\tau_{E\_}kinetic$ (hollow circle) (a) lower frequency branch, (b) higher frequency branch.

the exciting frequency of the applied electric potential remains in the 'kHz' range, the formation of a zero frequency zonal flow or other mechanisms like ***a*** ponderomotive force [22] effective at ICR frequencies, which may stabilize turbulent modes are not applicable. A possible candidate in relevant frequency range is GAM which can be driven through resonance from oscillating external currents [6, 20] that create time dependent poloidal flow shear. This produces turbulence suppression by the stochastic Doppler shift due to chaotic stretching of eddies [4]. Accordingly, the fluctuation level is reduced by a factor $(1+\tau_c\tau_{c,G}\langle k_\theta \tilde{V}_G^2\rangle)^{-1}$ which also applies for turbulent diffusion coefficient. It is then plausible to expect that high frequency biasing can excite GAM which do not damp as they would if not resonantly excited and they produce some sort of transport barrier that improves confinement. The idea was tested doing a simulation of the plasma evolution using 'ASTRA' transport code [21] with the modified turbulent transport coefficients. It has been run using parameters of the STOR-M tokamak in Ohmic heating regime where transport coefficients contain neoclassical as well as turbulent components. Drift wave turbulence can be affected by the high-frequency biasing potential as described above. A resonant electric field is produced by the electrode confined in a small radial region where turbulence reduction takes place. This would be effective when the driving frequency matches the GAM frequency in this edge region of STOR-M which is of the order of $f_{GAM} \sim c_s/R$ ~22kHz when T_e ~40 eV. The radial electric field is of the order of $E_r \sim V/\Delta_r \sim 6000$ V/m. A potential variation scale length of $\Delta_r \sim 1$cm was taken and the reduced anomalous diffusion coefficient for STOR-M is given by [4]

$$D = D_0\left(1+0.0012{E_r}^{2/3}f_G\right)^{-1} \quad (1)$$

where D_0 is the diffusion coefficient in absence of oscillating field and $f_G = \tau_c/\tau_{c,G}$, the ratio of correlation times for fluctuations and GAM. Here, $\tau_c = k_\perp^{-2/3} D^{-1/3} S_v^{2/3}$ was taken, with $k_\perp$ the radial mode extension assumed as 1 cm, $S_v \sim V/\Delta_r^2 B \sim 10^6 s^{-1}$ the velocity shear. The equilibrium diffusion coefficient is estimated as $D \sim 1\ m^2/s$. The parameter f_G is not known and is taken in the range 1-5. However, the GAM effect alone is not able to reproduce the complete phenomena, so another effect was included. This may come from an increased pinch velocity that confines particles against diffusion. Electrons traveling toroidally parallel to the magnetic field can be thrust by the electrode voltage every time when they pass through its region if the transit time matches the AC bias frequency. This allows the electrons to build a toroidal current which can give rise to a Ware-like radial pinch. It turns out that the electron toroidal rotation frequency for the drag velocity corresponding to the edge collisionality, $f_{tr} = eE/2\pi R m_e \nu_{ce}$, has a value ~ 20 kHz, matching the high frequency branch.

Both GAM and radial pinch are resonantly driven by AC voltage, the former producing turbulence and transport reduction while the later advects particles to the center. GAM is due to the oscillating radial electric field at the electrode that produces oscillating poloidal flow which reaches steady state at the driving frequency. As a result, a transport barrier is formed around the electrode.

These elements were incorporated in transport simulations considering different conditions for f_G. The results having a better agreement with experimental data correspond to choosing $f_G = 3$ for particle diffusion while $f_G = 5$ for thermal diffusivity. In this case there is an improvement of plasma confinement in the density while the electron temperature profile becomes less peaked. The results can be seen in figure 9, for a simulation in which the Ware pinch is increased by 12% during bias. The simulations were started by running the code without ac biasing until steady state was reached, having plasma parameters in agreement with typical STOR-M values and then the biasing was turned on. The evolution of representative plasma parameters given by ASTRA simulation can be observed in which the high-frequency potential of 22kHz with 60V is applied at time 0.08 s. It is clear that the behavior agrees in general terms with the discharge shown in figure 3. The average electron temperature $\langle \mathrm{T_e} \rangle$, radiated power from bremsstrahlung which would be detected in soft X-rays, average and central densities $\langle \mathrm{n_e} \rangle, \mathrm{n_{e0}}$ and τ_E are increased. Interestingly, particle flux to the wall which would be related to the H_α emission, shows very small changes which also agrees with the experimental outcomes. All these trends from simulation support the scenario of transport reduction by mode stabilization due to resonantly excited GAM associated with high-frequency biasing potential.

According to our knowledge, this is the first time experimental studies of high frequency biasing in 'kHz' range have been performed in a tokamak. Previously,

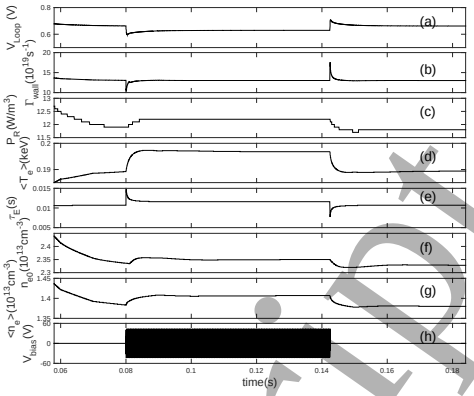

FIG. 9: Simulation time evolution of STOR-M discharge of (a) loop voltage, (b) particle flux to wall, (c) radiated power, (d) average electron temperature, (e) energy confinement time, (f) central plasma density, (g) average plasma density, (h) high frequency AC bias voltage of 22 kHz.

elaborate experimental studies of DC biasing through electrode and limiter [11, 23] were performed in STOR-M. Those experiments show that improved confinement happens at +150V & -350V with electrode current $\sim$ 22A. The present high frequency biasing experiments show that improved confinement can be achieved with a triangular pulse of $\pm 60V$ with bias current from -24A to +2A at 1kHz-5kHz & 20kHz-25kHz frequency regimes. The kinetic τ_E increases by 40% and 20% for lower & higher frequency branches respectively. τ_p is also enhanced around 25% in both frequency regimes. Also, soft X ray emission is enhanced in the central part of the plasma column, an indication of central energy density enhancement. The simulation of the proposed model also shows same trend of observed results at higher frequency regimes(20-25)kHz. So, a physical explanation for improved confinement at higher frequency regimes may be due to resonant GAM excitation combined with a radial (Ware) pinch produced by the toroidal transit electron current resonantly driven at the bias frequency around 22 kHz. In this experiment, fluctuation studies and flow measurements have not been carried out and remains an important future study for further clarification of the physical mechanism and its simulation modeling for the improved confinement.

Acknowledgments

We would like to acknowledge NSERC for supporting this work. We also would like to acknowledge the machine workshop in our Physics Department. Special thanks go to Mr. Chomyshen and Mr. Toporowski in the machine workshop for their kind help and friendly approach when needed. The work of A.V. Melnikov was supported by Russian Science Foundation, project

no. 19-12-00312 and in part by the Competitiveness Programme of the National Research Nuclear University "MEPhI". JJM was supported by projects PAPIIT IN112118 and Conacyt A1-S-24157.

I. REFERENCES:

[1] G. Van Oost et.al., Plasma Phys. Control. Fusion **45**, 621 (2003)
[2] Ch. P. Ritz, R. D. Bengtson, et.al., Phys. Fluids **27**, 2956 (1984)
[3] P. C. Liewer, J. M. McChesney, et.al., Phys. Fluids **29**, 309 (1986)
[4] P.H. Diamond, et.al., Plasma Phys. Control Fusion **47**, R35 (2005)
[5] Debjyoti Basu, et.al., Nucl. Fusion **58**, 024001 (2018)
[6] R. V. Shurygin and A. V. Melnikov, Plasma Physics Reports **44**, 303(2018)
[7] R. J. Taylor, et.al., Phys. Rev. Letter **63** 2365 (1989)
[8] R. R. Weynants, et.al., Nucl. Fusion **32** 837 (1992)
[9] Debjyoti Basu, et.al., Physics of Plasmas **19** 072510 (2012)
[10] A.V. Melnikov,et.al., Fusion Science and Technology **46**, 299(2004)
[11] C. Xiao et al., Physics of Plasmas **1**, 2291 (1994)
[12] C. Silva et al., Plasma Phys. Control. Fusion **46** 163 (2004)
[13] Zhai Kan et al., Physical Review E **55** 3431 (1997)
[14] T. UCKAN et al., Nucl. Fusion **35**, 487 (1995)
[15] J. W. Brooks, et.al., Review of Scientific Instruments **90**, 023503 (2019)
[16] C. Xiao, et.al., Review of Scientific Instruments **79**, 10E926 (2008)
[17] J. A. Heikkinen, Physics of Plasmas **8** 2824 (2001)
[18] C. Hidalgo, et.al., Plasma Phys. Control. Fusion **46** 287 (2004)
[19] E.H. Silver et al., Review of Scientific Instruments **53** 1198 (1982)
[20] C.P. Hung and A.B. Hassam, Physics of Plasmas **20**, 092107 (2013)
[21] G. V. Pereverzev, P. N. Yushmanov, ASTRA: Automated System for TRansport Analysis (Max-Plank-Institute fr Plasmaphysik Rep IPP vol 5/98) (Garching: IPP) (2002)
[22] J.J. Martinell, et al., Radiation Effects and Defects in Solids **168**, 866 (2013)
[23] W. Zhang, et al., Phys. Fluids B **4**, 3277 (1992)